



Published in final edited form as:

*Nat Med.* 2011 April ; 17(4): 500–503. doi:10.1038/nm.2344.

## Subtypes of Pancreatic Ductal Adenocarcinoma and Their Differing Responses to Therapy

Eric A. Collisson<sup>1,2,\*</sup>, Anguraj Sadanandam<sup>1,7,\*</sup>, Peter Olson<sup>3,8</sup>, William J. Gibb<sup>1,9</sup>, Morgan Truitt<sup>3</sup>, Shenda Gu<sup>1</sup>, Janine Cooc<sup>6</sup>, Jennifer Weinkle<sup>1</sup>, Grace E. Kim<sup>4</sup>, Lakshmi Jakkula<sup>1</sup>, Heidi S. Feiler<sup>1</sup>, Andrew H. Ko<sup>2</sup>, Adam B. Olshen<sup>5</sup>, Kathleen L. Danenberg<sup>6</sup>, Margaret A. Tempero<sup>2</sup>, Paul T. Spellman<sup>1</sup>, Douglas Hanahan<sup>3,7</sup>, and Joe W. Gray<sup>1,10,†</sup>

<sup>1</sup>Life Sciences Division, Lawrence Berkeley National Laboratory, Berkeley, CA 94720, USA

<sup>2</sup>Division of Hematology and Oncology, Diabetes Center, University of California, San Francisco, CA 94143, USA <sup>3</sup>Department of Biochemistry and Biophysics, University of California, San Francisco, CA 94143, USA <sup>4</sup>Department of Pathology, University of California, San Francisco, CA 94143, USA <sup>5</sup>Department of Epidemiology and Biostatistics and Helen Diller Family Comprehensive Cancer Center, University of California, San Francisco, CA 94143, USA

<sup>6</sup>Response Genetics Inc., Los Angeles, CA 90033, USA <sup>7</sup>Swiss Institute for Experimental Cancer Research (ISREC), Swiss Federal Institute of Technology Lausanne (EPFL), Lausanne CH-1015, Switzerland <sup>10</sup>Biomedical Engineering, Oregon Health and Science University

Pancreatic ductal adenocarcinoma (PDA) is a lethal disease. Overall survival is typically six months from diagnosis<sup>1</sup>. Numerous phase III trials of agents effective in other malignancies have failed to benefit unselected PDA populations, although patients do occasionally respond. Studies in other solid tumors have shown that heterogeneity in response is determined, in part, by molecular differences between tumors. Further, treatment outcomes are improved by targeting drugs to tumor subtypes in which they are selectively effective, with breast<sup>2</sup> and lung<sup>3</sup> cancers providing recent examples. Identification of PDA molecular subtypes has been frustrated by a paucity of tumor specimens available for study. We have overcome this problem by combined analysis of transcriptional profiles of primary PDA samples from several studies along with human and mouse PDA cell lines. We define three PDA subtypes: classical, quasi-mesenchymal, and exocrine-like, and present evidence for clinical outcome and therapeutic response differences between them. We further define gene signatures for these subtypes that may have utility in stratifying patients for treatment and

Users may view, print, copy, download and text and data- mine the content in such documents, for the purposes of academic research, subject always to the full Conditions of use: [http://www.nature.com/authors/editorial\\_policies/license.html#terms](http://www.nature.com/authors/editorial_policies/license.html#terms)

<sup>†</sup>Corresponding Author: Biomedical Engineering, 3303 SW Bond Ave., CH13B, Portland, OR 97239 Tel: 503-494-6500, Fax: 503-418-9311 [grayjo@ohsu.edu](mailto:grayjo@ohsu.edu).

<sup>\*</sup>Equal Contributors

<sup>8</sup>Current Address: Pfizer, 10724 Science Center Drive, La Jolla, CA 92121

<sup>9</sup>Current Address: Genomic Health, 301 Penobscot Drive, Redwood City, CA 94063

### Author Contributions:

E.A.C. and A.S. designed, conducted and interpreted experiments, and wrote the manuscript. P.O., W.J.G, M.T., S.G., J.C., J.W., L.J., and H.S.F. performed experiments. K.L.D., and P.T.S. provided support and interpreted experiments. G.E.K. and A.H.K. coordinated clinical sample acquisition. A.B.O. provided statistical expertise. M.A.T provided support, interpreted experiments and coordinated clinical sample acquisition. D.H. and J.W.G. designed and interpreted experiments, wrote the manuscript and supervised the project.

present preclinical model systems that may be used to identify new subtype specific therapies.

Global gene expression analysis has proved useful for subtype identification in many human tumor types<sup>4</sup>. We approached PDA subtype identification by first identifying intrinsically variable (standard deviation > 0.8) genes in two gene expression microarray datasets from resected PDA. We generated one dataset using microdissected PDA material (UCSF tumors, n=27) from clinical samples for which information on survival duration was available and the second was previously published (Badea, et al.)<sup>5</sup>. To increase power, we merged these two datasets using the distance weighted discrimination (DWD) method<sup>6,7</sup> and included intrinsically variable genes common to both studies. We then performed nonnegative matrix factorization (NMF) analysis with consensus clustering<sup>8</sup> to identify subtypes of the disease. This analysis supported up to three subtypes (cophenetic coefficient >0.99; Supplementary Figs. 1, 2a and Supplementary Tables 1–3). We then developed a gene signature by using subtypes defined in NMF analysis of the merged clinical datasets to supervise significance analysis of microarrays (SAM) analysis<sup>9</sup> with false discovery rate (FDR) less than 0.001. This resulted in a 62 gene signature, designated *PDAAssigner*. The three PDA subtypes in the merged clinical dataset and their expression of *PDAAssigner* genes are shown in Fig. 1a. We designated these subtypes as classical, quasi-mesenchymal (QM-PDA) and exocrine-like, based on our interpretation of subtype specific gene expression. The classical subtype had high expression of adhesion-associated and epithelial genes, the QM-PDA subtype showed high expression of mesenchyme associated genes. The exocrine-like subtype showed relatively high expression of tumor cell derived digestive enzyme genes, with immunohistochemical staining supporting this observation (Supplementary Fig. 3). Analysis of *PDAAssigner* gene expression in three additional published PDA expression datasets of unique origin, platform or processing<sup>10–12</sup> also supported these three subtypes (Supplementary Fig. 4) demonstrating the robust nature of the subtype classification in early stage PDA.

Survival after PDA resection has been associated with many factors including stage (tumor size and nodal involvement) and grade (degree of differentiation)<sup>13</sup>, but no one factor has been consistently prognostic<sup>14,15</sup>. We found that stratification by PDA transcriptional subtype provided useful prognostic information in one PDA dataset (UCSF) for which clinical annotation was available. Specifically, patients with classical subtype tumors fared better than patients with QM-PDA subtype tumors after resection (p=0.038, log rank, Fig. 1b). In this same data set, stage and grade were not significantly related (p>0.99), stage was not significantly associated with subtype (p=0.40), while grade was (p=0.041) (univariate analyses). In a multivariate Cox regression model including stage and subtype, subtype was an independent predictor of overall survival (p=0.024) indicating that PDA subtype independently contributed prognostic information to pathological staging in PDA. Associations of PDA subtype with other clinical variables are summarized in Supplementary Table 4. This analysis supports the use of subtypes (as defined using *PDAAssigner*) as an independent prognostic indicator in resected PDA.

Further validation of PDA subtypes and preclinical identification of subtype specific therapeutic agents would be facilitated by the availability of laboratory models of the

subtypes. Therefore, we asked if the PDA subtypes were represented in a collection of 19 human and 15 mouse PDA cell lines. The 19 human PDA cell lines were selected from publicly available PDA lines while the 15 mouse lines were derived by us from genetically engineered *Tp53*<sup>-/-</sup> and *INK4A*<sup>-/-16</sup> models of PDA. The analyses of the human and mouse PDA cell lines using the 62 *PDAAssigner* genes are shown in Fig. 1c,d, as well as in Supplementary Figs. 2b–e. Supplementary Tables 5 and 6. These cell line collections contain representatives of the classical and QM-PDA subtypes, but not the exocrine-like subtype. The absence of the exocrine-like subtype in the cell line collection raises the possibility that this subtype is an artifact of contaminating normal pancreas tissue adjacent to tumor. However, the UCSF samples were prepared by microdissection to enrich for PDA cancer cells thereby minimizing contaminating tumor-associated stroma and/or adjacent normal exocrine pancreas. This dataset includes the exocrine-like subtype, which argues that it is a *bona fide* PDA subtype. Thus, we conclude that the cell line collections model two of the PDA subtypes thereby enabling exploration of biological differences between these two PDA subtypes and may facilitate screening for classical and QM-PDA subtype-specific therapeutic agents and biological properties.

Two genes associated with PDA subtypes, GATA binding protein 6 (*GATA6*) and v-ki-ras2 Kirsten rat sarcoma viral oncogene homolog (*KRAS*), two variable genes in our UCSF PDA dataset, Supplementary Table 1a), have been implicated in both aspects of normal development and cancer pathophysiology in published studies. GATA-family transcription factors are associated with tissue specific differentiation and have been demonstrated to be subtype specific markers in other cancers. For example, GATA binding protein 3 (*GATA3*) is required for luminal differentiation in the breast<sup>17</sup>, and high *GATA3* characterizes luminal subtype breast cancers<sup>18</sup>. Likewise, *GATA6* is essential for pancreatic development<sup>19</sup> and has been implicated in PDA<sup>20,21</sup>. *GATA6* is highly expressed in most classical subtype tumors and cell lines, and comparatively low in the QM-PDA cell lines and tumors. Additionally, a previously published gene signature associated with *GATA6* overexpression<sup>20</sup> is enriched in the classical subtype (Supplementary Fig. 5). Seeking to establish a possible functional role underlying the observed differences in *GATA6* expression, we assessed the impact of *GATA6*-directed RNAi knockdown on colony formation in soft agar in the classical and QM-PDA cell lines. *GATA6* depletion impaired anchorage-independent growth in classical PDA cell lines, but not in QM-PDA cell lines (Fig. 2), consistent with a functional, subtype-specific role for this transcription factor in the classical PDA subtype.

Recent work in the mouse demonstrates that PDA can arise from a variety of precursor cells by activating *KRAS* in distinct cellular compartments of the pancreas<sup>22</sup>. Others have found that cancer cell lines harboring mutant *KRAS* differ in their dependence on *KRAS*<sup>23</sup>. These findings imply plasticity in either reliance on *KRAS* signaling or a cell-type specific role for mutant *KRAS* in different cells of origin/lineages in PDA, or both. They further suggested to us that despite *KRAS* mutation in most PDAs, *KRAS* dependence might differ by PDA subtype. We found *KRAS* mRNA levels elevated in classical subtype PDAs relative to the other subtypes (Supplementary Fig. 6,  $p < 0.05$  in UCSF samples). We explored the relationship between *KRAS* dependence and subtype by using RNAi to probe *KRAS*-mutant

human PDA cell lines for dependence on *KRAS*. Classical PDA lines proved to be relatively more dependent on *KRAS* than QM-PDA lines (Fig. 3). Further, a previously reported signature of *KRAS*-addiction<sup>23</sup> is enriched in the classical subtype (Supplementary Fig. 7). These results suggest that *KRAS*-directed therapy, while not yet a clinical reality, might be best deployed in classical PDA. Mouse models capable of sequentially activating and then deleting mutant *KRAS* would further these observations to genetically define the respective roles mutant *KRAS* plays in both the initiation and ongoing maintenance of PDA.

We tested the possibility that PDA subtypes with different biological characteristics might have subtype-specific drug responses by measuring responses to gemcitabine and erlotinib (the backbone of current treatment regimens<sup>24</sup>) in human PDA cell lines of known subtype. QM-PDA subtype lines were, on average, more sensitive to gemcitabine than the classical subtype (Fig. 4). Conversely, erlotinib was more effective in classical subtype cell lines. This suggests that *KRAS* mutation status is an imperfect predictor of sensitivity to EGFR-targeted therapy in PDA, an observation consistent with findings in nonsmall cell lung<sup>25</sup> and colorectal cancers<sup>26</sup>, and implies that cancer cells dependent on mutant *KRAS* still employ the EGFR to some extent. These results further establish phenotypic differences between the classical and QM-PDA subtypes, and suggest that these and perhaps additional drugs will show subtype specificity in PDA, a distinction that could be exploited in clinical trial sensitivity enrichment schemes. More immediately, these results indicate that gemcitabine and erlotinib are preferentially active in different PDA subtypes, so that the current practice of combining them may increase toxicity without increasing efficacy for many patients. Combining agents with similar subtype specificity might be considered instead.

In summary, our data support the existence of three intrinsic subtypes of PDA that progress at different rates clinically and may respond differently to selected therapies. The validity of these subtypes is supported by analysis of multiple primary clinical datasets as well as of PDA cell lines both from human tumors and from mouse models engineered with the hallmark genetic lesions of human PDA. Knowledge of these subtypes may motivate investigation of associations between clinico-pathologic variables and these subtypes by collaborative consortia examining the molecular diversity of PDA<sup>27</sup>. The markers that define these subtypes may have prognostic utility in risk-adapted surgical approaches<sup>28</sup> or predictive utility in sensitivity enrichment schemes. The use of subtyped human and mouse PDA preclinical models promises to accelerate identification of subtype specific functional and regulatory processes that can be exploited to therapeutic benefit. In turn, such assay systems could be used to screen therapeutic approaches, empirically or based on mechanism, to identify those that are potent against PDA, either in a specific subtype that would then be used to personalize treatment<sup>29</sup>, or spanning the subtypes with possible therapeutic generality.

## Methods

### Clinical Samples

After institutional review board approval, we selected archival material from pancreatic ductal adenocarcinoma resections performed at the University of California, San Francisco

between 1993 and 2006. G.E.K. reviewed all cases prior to inclusion in the study. Tissue processing is described in Supplementary Methods.

### Merging of Microarray Datasets

After processing of microarrays (as described in Supplementary Information), we screened the UCSF and Badea et al.,<sup>5</sup> PDA datasets separately by selecting probes with standard deviation (SD) > 0.8. We then merged SD-selected datasets using DWD<sup>7</sup> as described<sup>6</sup>. We column (samples) normalized to N(0,1) and row (probe or gene) normalized each dataset by median centering. We merged the processed datasets using DWD and finally, we median centered the rows.

### NMF and SAM Analysis

We analyzed the merged datasets by consensus clustering-based NMF<sup>8</sup> to identify stable subtypes using R code from GenePattern<sup>30</sup>. See supplement for details regarding the interpretation of subtypes derived from consensus-based NMF clustering. We identified *PDAAssigner* genes using three-class SAM analysis based on classes identified from NMF analysis using the Bioconductor<sup>31</sup> package, Siggenes, and generated heatmaps of samples by *PDAAssigner* genes using Cluster software<sup>32</sup>. For cell line classification, we merged the cell line datasets with core PDA clinical datasets after selection of the 62 *PDAAssigner* genes from each dataset followed by DWD based merging. We visualized datasets using the Hierarchical Clustering Viewer (HCV) from GenePattern<sup>30</sup>.

### Clinical Outcome Analysis

We calculated overall survival in days from the time of PDA resection until date of death as defined by the State of California Death Registry and clinical records. We employed the log-rank test for univariate associations with survival or the Cox proportional hazards model for multivariate modeling of survival. We applied Fisher's exact test to investigate the relationships among subtype, stage and grade. We used the R language for all analyses. We drew the survival curve using web-based GenePattern<sup>30</sup>.

### Drug Sensitivity

We plated  $2.5 \times 10^3$  cells per well on day 0, treated with erlotinib or gemcitabine in nine, five-fold serial dilutions on day 1 and estimated cell number using Cell Titre Glow assay (CTG, Promega) on day 4. IC<sub>50</sub> was calculated using the Calcsyn program (Biosoft).

### RNAi

We obtained validated pLKO-based shRNA vectors shKRAS#5<sup>33</sup> from Dr. B.R. Stockwell (NYU) and shGATA6#5, and shLuc<sup>34</sup> from Dr. R Adam, (Boston Children's Hospital). We packaged lentiviruses, transduced cells and then selected in puromycin for 48 hours. For shKRAS proliferation experiments, we plated  $2.5 \times 10^3$  transduced cells per well on day 0 in 96 well plates, then counted one plate on day one and the other plate on day four. We confirmed protein knockdown by western blotting using the Odyssey system, with 10ug per lane of total protein and the c19 KRas antibody (Santa Cruz), normalized to total actin (I-19, Santa Cruz) and compared to pLKOshLuc -KRas levels. For *GATA6* knockdown

experiments, after puromycin selection cells we trypsinized and plated transduced cells in soft agar as described<sup>35</sup>. We assessed *GATA6* transcript levels on the day of plating in soft agar as described<sup>34</sup>.

See Supplementary Information for detailed methods.

## Supplementary Material

Refer to Web version on PubMed Central for supplementary material.

## Acknowledgments

We are grateful to M. Lenburg, the Gray, Hanahan, and Speed labs for discussion. We thank L. Chin (Dana-Farber Cancer Institute), S. Batra (University of Nebraska Medical Center), M. McMahon (University of California San Francisco) and A. Singh (Massachusetts General Hospital) for cell lines, and B. Stockwell (New York University) and R. Adam (Children's Hospital Boston) for shRNA. E.A.C was supported by a Young Investigator Award from the American Society of Clinical Oncology and US National Cancer Institute (NCI) K08 CA137153. A.S. was supported by Department of Defense (DOD) Postdoctoral Fellowship (BC087768). The research in the laboratory of D.H. was supported by a NCI Program Project Grant PO1 CA 117969; D.H. is an American Cancer Society Research Professor. This work was supported by the Director, Office of Science, Office of Biological & Environmental Research, of the United States Department of Energy under Contract No. DE-AC02-05CH11231, by the NIH/NCI grants P50 CA 58207, P50 CA 83639 and by the U54 CA 112970 to J.W.G.

## References

1. Stathis A, Moore MJ. Advanced pancreatic carcinoma: current treatment and future challenges. *Nat Rev Clin Oncol*. 2010; 7:163–172. [PubMed: 20101258]
2. Slamon DJ, et al. Use of chemotherapy plus a monoclonal antibody against HER2 for metastatic breast cancer that overexpresses HER2. *N Engl J Med*. 2001; 344:783–792. [PubMed: 11248153]
3. Lynch TJ, et al. Activating mutations in the epidermal growth factor receptor underlying responsiveness of non-small-cell lung cancer to gefitinib. *N Engl J Med*. 2004; 350:2129–2139. [PubMed: 15118073]
4. Alizadeh AA, et al. Distinct types of diffuse large B-cell lymphoma identified by gene expression profiling. *Nature*. 2000; 403:503–511. [PubMed: 10676951]
5. Badea L, Herlea V, Dima SO, Dumitrascu T, Popescu I. Combined gene expression analysis of whole-tissue and microdissected pancreatic ductal adenocarcinoma identifies genes specifically overexpressed in tumor epithelia. *Hepatogastroenterology*. 2008; 55:2016–2027. [PubMed: 19260470]
6. Herschkowitz JI, et al. Identification of conserved gene expression features between murine mammary carcinoma models and human breast tumors. *Genome Biol*. 2007; 8:R76. [PubMed: 17493263]
7. Benito M, et al. Adjustment of systematic microarray data biases. *Bioinformatics*. 2004; 20:105–114. [PubMed: 14693816]
8. Brunet JP, Tamayo P, Golub TR, Mesirov JP. Metagenes and molecular pattern discovery using matrix factorization. *Proc Natl Acad Sci U S A*. 2004; 101:4164–4169. [PubMed: 15016911]
9. Tusher VG, Tibshirani R, Chu G. Significance analysis of microarrays applied to the ionizing radiation response. *Proc Natl Acad Sci U S A*. 2001; 98:5116–5121. [PubMed: 11309499]
10. Balagurunathan Y, et al. Gene expression profiling-based identification of cell-surface targets for developing multimeric ligands in pancreatic cancer. *Mol Cancer Ther*. 2008; 7:3071–3080. [PubMed: 18765825]
11. Pei H, et al. FKBP51 affects cancer cell response to chemotherapy by negatively regulating Akt. *Cancer Cell*. 2009; 16:259–266. [PubMed: 19732725]
12. Grutzmann R, et al. Gene expression profiling of microdissected pancreatic ductal carcinomas using high-density DNA microarrays. *Neoplasia*. 2004; 6:611–622. [PubMed: 15548371]

13. Brennan MF, Kattan MW, Klimstra D, Conlon K. Prognostic nomogram for patients undergoing resection for adenocarcinoma of the pancreas. *Ann Surg.* 2004; 240:293–298. [PubMed: 15273554]
14. Biankin AV, et al. Expression of S100A2 Calcium-Binding Protein Predicts Response to Pancreatectomy for Pancreatic Cancer. *Gastroenterology.* 2009
15. Blackford A, et al. SMAD4 gene mutations are associated with poor prognosis in pancreatic cancer. *Clin Cancer Res.* 2009; 15:4674–4679. [PubMed: 19584151]
16. Bardeesy N, et al. Both p16(Ink4a) and the p19(Arf)-p53 pathway constrain progression of pancreatic adenocarcinoma in the mouse. *Proc Natl Acad Sci U S A.* 2006; 103:5947–5952. [PubMed: 16585505]
17. Kouros-Mehr H, Slorach EM, Sternlicht MD, Werb Z. GATA-3 maintains the differentiation of the luminal cell fate in the mammary gland. *Cell.* 2006; 127:1041–1055. [PubMed: 17129787]
18. Mehra R, et al. Identification of GATA3 as a breast cancer prognostic marker by global gene expression meta-analysis. *Cancer Res.* 2005; 65:11259–11264. [PubMed: 16357129]
19. Decker K, Goldman DC, Grash CL, Sussel L. Gata6 is an important regulator of mouse pancreas development. *Dev Biol.* 2006; 298:415–429. [PubMed: 16887115]
20. Kwei KA, et al. Genomic profiling identifies GATA6 as a candidate oncogene amplified in pancreatobiliary cancer. *PLoS Genet.* 2008; 4:e1000081. [PubMed: 18535672]
21. Fu B, Luo M, Lakkur S, Lucito R, Iacobuzio-Donahue CA. Frequent genomic copy number gain and overexpression of GATA-6 in pancreatic carcinoma. *Cancer Biol Ther.* 2008; 7:1593–1601. [PubMed: 18769116]
22. Gidekel Friedlander SY, et al. Context-dependent transformation of adult pancreatic cells by oncogenic K-Ras. *Cancer Cell.* 2009; 16:379–389. [PubMed: 19878870]
23. Singh A, et al. A gene expression signature associated with “K-Ras addiction” reveals regulators of EMT and tumor cell survival. *Cancer Cell.* 2009; 15:489–500. [PubMed: 19477428]
24. Moore MJ, et al. Erlotinib plus gemcitabine compared with gemcitabine alone in patients with advanced pancreatic cancer: a phase III trial of the National Cancer Institute of Canada Clinical Trials Group. *J Clin Oncol.* 2007; 25:1960–1966. [PubMed: 17452677]
25. Yauch RL, et al. Epithelial versus mesenchymal phenotype determines in vitro sensitivity and predicts clinical activity of erlotinib in lung cancer patients. *Clin Cancer Res.* 2005; 11:8686–8698. [PubMed: 16361555]
26. De Roock W, et al. Association of KRAS p.G13D mutation with outcome in patients with chemotherapy-refractory metastatic colorectal cancer treated with cetuximab. *Jama.* 2010; 304:1812–1820. [PubMed: 20978259]
27. International network of cancer genome projects. *Nature.* 2007; 464:993–998.
28. Raut CP, Evans DB, Crane CH, Pisters PW, Wolff RA. Neoadjuvant therapy for resectable pancreatic cancer. *Surg Oncol Clin N Am.* 2004; 13:639–661. ix. [PubMed: 15350939]
29. McDermott U, et al. Identification of genotype-correlated sensitivity to selective kinase inhibitors by using high-throughput tumor cell line profiling. *Proc Natl Acad Sci U S A.* 2007; 104:19936–19941. [PubMed: 18077425]
30. Kuehn H, Liberzon A, Reich M, Mesirov JP. Using GenePattern for gene expression analysis. *Curr Protoc Bioinformatics.* 2008; Chapter 7(Unit 7):12. [PubMed: 18551415]
31. Gentleman RC, et al. Bioconductor: open software development for computational biology and bioinformatics. *Genome Biol.* 2004; 5:R80. [PubMed: 15461798]
32. Eisen MB, Spellman PT, Brown PO, Botstein D. Cluster analysis and display of genome-wide expression patterns. *Proc Natl Acad Sci U S A.* 1998; 95:14863–14868. [PubMed: 9843981]
33. Yagoda N, et al. RAS-RAF-MEK-dependent oxidative cell death involving voltage-dependent anion channels. *Nature.* 2007; 447:864–868. [PubMed: 17568748]
34. Kanematsu A, Ramachandran A, Adam RM. GATA-6 mediates human bladder smooth muscle differentiation: involvement of a novel enhancer element in regulating alpha-smooth muscle actin gene expression. *Am J Physiol Cell Physiol.* 2007; 293:C1093–1102. [PubMed: 17626241]

35. Collisson EA, De A, Suzuki H, Gambhir SS, Kolodney MS. Treatment of metastatic melanoma with an orally available inhibitor of the Ras-Raf-MAPK cascade. *Cancer Res.* 2003; 63:5669–5673. [PubMed: 14522881]

Author Manuscript

Author Manuscript

Author Manuscript

Author Manuscript



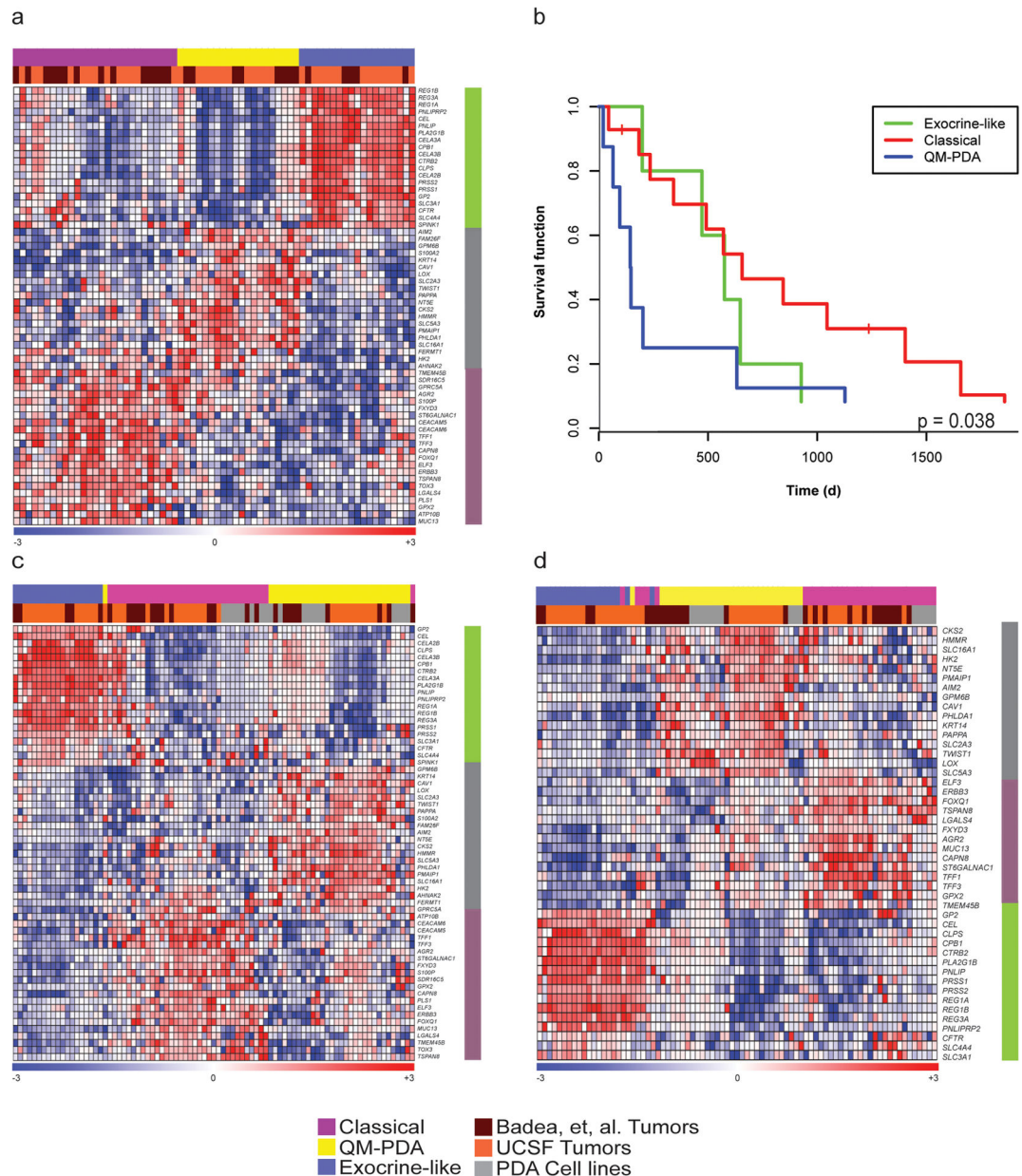


**Figure 1. Subtypes of PDA in tumors and cell lines and their prognostic significance**  
**A.** Heatmap (HM) showing three subtypes of PDA in a DWD-merged UCSF and Badea et al.<sup>5</sup> PDA microarray datasets using the *PDAssigner* geneset. **B.** Kaplan-Meier Survival curve comparing survival of classical (red), QM-PDA (blue) and exocrine-like (green) subtype patients. Survival time is in days (d). p-value is by Log-rank test. **C.** HM showing three subtypes of PDA in a DWD-merged core clinical and human PDA cell line microarray datasets using the *PDAssigner* geneset. **D.** HM showing three subtypes of PDA in a DWD-merged core clinical PDA and mouse PDA cell line microarray datasets using *PDAssigner* geneset. In the top bar, magenta marks classical subtype PDA, yellow marks QM-PDA and light blue marks exocrine-like (by NMF). The second from top bar denotes sample set of origin, with brown samples originating from UCSF, orange samples originating from Badea

et al.<sup>5</sup> PDA datasets and gray samples originating from either human (C) or mouse (D) PDA cell lines. The bars on the side denote *PDAAssigner* genes upregulated in classical (violet), QM-PDA (gray) and exocrine-like (green).

Author Manuscript

Author Manuscript

Author Manuscript

Author Manuscript

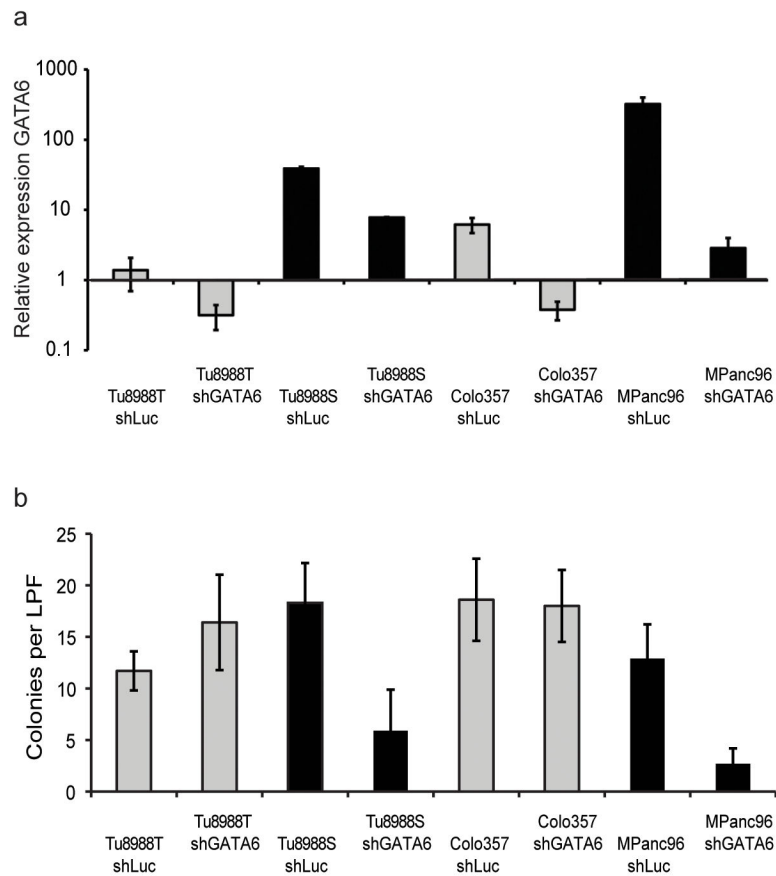


**Figure 2. Classical PDA subtype and the *GATA6* transcription factor**

**A.** Relative log expression of *GATA6* in PDA cell lines, transduced with shRNA against *GATA6* or control, was determined by qRT-PCR. Black columns are classical lines, gray columns are QM-PDA lines, note log scale. **B.** Colonies per Low Powered Field (LPF) in PDA cell lines transduced with shRNA against *GATA6* or control.

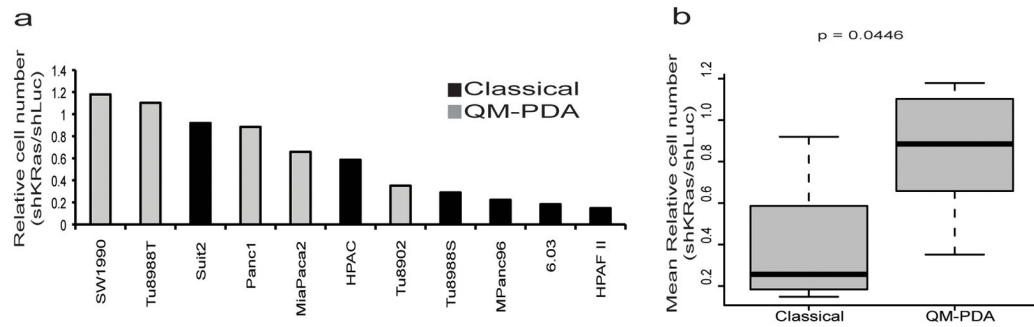


**Figure 3. Classical subtype cells depend on KRAs**

**A.** PDA lines (all with GTPase inactivating *KRAS* mutations), were transduced with lentiviruses encoding either control (shLUC) or *KRAS* (shKRAs) directed RNAi. Relative proliferation is plotted. Black columns are classical lines and gray columns are QM-PDA lines. **B.** Box plot of relative proliferation of classical and QM-PDA human PDA cell lines. p-values by the Kruskal-Wallis test.

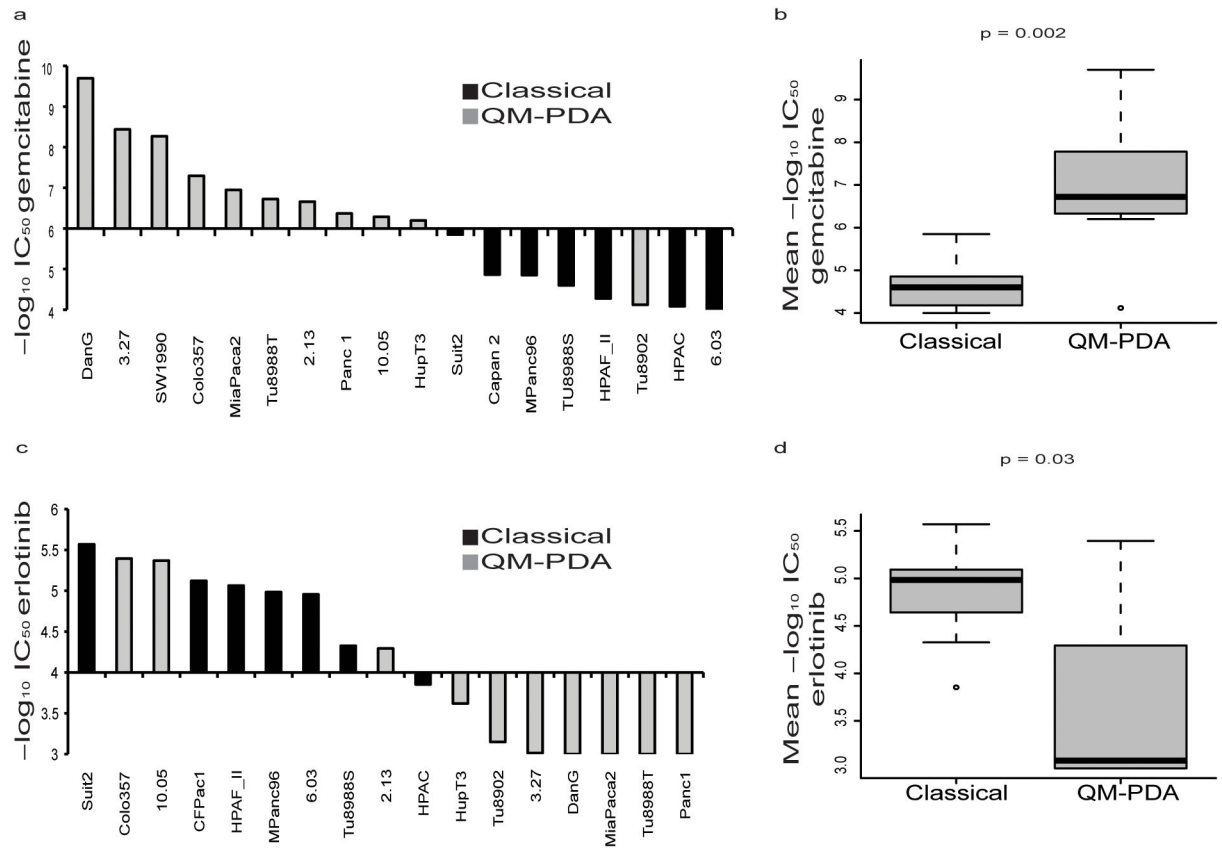


**Figure 4. Drug Responses Differ by Subtype**

$IC_{50}$  in negative  $\log_{10}$  of drug concentration is plotted for each cell line tested with **A.** gemcitabine and **C.** erlotinib. Black columns are classical lines and gray columns are QM-PDA lines. Box Plot of  $IC_{50}$  of classical and QM-PDA human PDA cell lines for **B.** gemcitabine and **D.** erlotinib, p-values represent statistics using Kruskal-Wallis test.